

Ethanol inhibits L1 cell adhesion molecule tyrosine phosphorylation and dephosphorylation and activation of pp60^{src}

Natalie K. Yeane^{*}, Min He[†], Ningfeng Tang[†], Alfred T. Malouf[‡], Mary Ann O'Riordan[§], Vance Lemmon[¶] and Cynthia F. Bearer[†]

^{*}Department of Pediatrics, Addenbrookes Hospital, Cambridge, UK

[†]Department of Pediatrics, University of Maryland School of Medicine, Baltimore, Maryland, USA

[‡]Department of Pediatrics, University Hospitals of Cleveland, Cleveland, Ohio, USA

[§]NineSigma, Inc., Cleveland, Ohio, USA

[¶]The Miami Project to Cure Paralysis, University of Miami Miller School of Medicine, Miami, Florida, USA

Abstract

Fetal alcohol syndrome is a leading cause of mental retardation. The neuropathology found in patients with fetal alcohol syndrome overlaps with those with mutations in the gene for cell adhesion molecule (L1). We have previously shown that L1-mediated neurite outgrowth and L1 activation of extracellular receptor kinases 1/2 are inhibited at low concentrations of ethanol. One possible mechanism for this effect is through disruption of a tyrosine-based sorting signal, Y(1176)RSLE, on the cytoplasmic domain of L1. Our goal was to determine if ethanol inhibited the sorting signal or its phosphorylation state. Using cerebellar granule neurons and dorsal root ganglion neurons, we found that ethanol had no effect on L1 distribution to the growth cone or its ability to be expressed on the cell surface as determined by confocal microscopy. In cerebellar

granule neurons, clustering of L1 resulted in increased dephosphorylation of Y(1176), increased L1 tyrosine phosphorylation, and an increase in the activation of pp60^{src} as measured by immunoblot. All changes were inhibited by 25 mM ethanol. Using PP2 to inhibit pp60^{src} activation resulted in inhibition of increases in L1 tyrosine and extracellular receptor kinases 1/2 phosphorylation, and Y(1176) dephosphorylation. We conclude that ethanol disrupts L1 trafficking/signaling following its expression on the surface of the growth cone, and prior to its activation of pp60^{src}.

Keywords: ethanol, fetal alcohol syndrome, L1 cell adhesion molecule, pp60^{src}, tyrosine dephosphorylation, tyrosine phosphorylation.

J. Neurochem. (2009) 10.1111/j.1471-4159.2009.06143.x

Fetal exposure to ethanol during nervous system development is the leading known cause of mental retardation (Stratton *et al.* 1996). Many of the anatomic brain anomalies described in fetal alcohol syndrome are also observed in syndromes caused by mutations in the gene for a neural cell adhesion molecule (NCAM) (L1). The neuromigrational defects found in both conditions include hydrocephalus, absence of the corpus callosum, and cerebellar dysplasia (Roebuck *et al.* 1998). The striking correlation between ethanol induced neurological defects and anomalies resulting from defective L1 has led to speculation that disruption of L1 function may be one mechanism by which ethanol exerts teratogenicity on the nervous system (Charness *et al.* 1994; Bearer 2001). Previous work has shown that L1-mediated neurite outgrowth is inhibited by ethanol (Bearer *et al.* 1999; Watanabe *et al.* 2004). Further, we have shown that L1 activation of extracellular receptor kinases 1/2 (ERK1/2) is

also inhibited by ethanol (Tang *et al.* 2006). These results support the hypothesis that ethanol's effect on L1 function are at least partially responsible for the neurodevelopmental

Received January 22, 2009; revised manuscript received March 13, 2009; accepted April 27, 2009.

Address correspondence and reprint requests to Cynthia F. Bearer, Department of Pediatrics, University of Maryland Hospital for Children, 29 S. Greene St., GS110, Baltimore, MD 21201, USA.

E-mail: cbearer@peds.umaryland.edu

Abbreviations used: BSA, bovine serum albumin; CGN, cerebellar granule neurons; DMEM, Dulbecco's modified Eagle's medium; DMSO, dimethylsulfoxide; DRG, dorsal root ganglion; ERK1/2, extracellular receptor kinases 1/2; FBS, fetal bovine serum; HBSS, Hank's balanced salt solution; HRP, horseradish peroxidase; L1, cell adhesion molecule; LCD, cytoplasmic domain of L1; L1-Fc, a chimeric protein consisting of the extracellular domain of L1 and the Fc domain of IgG; MAP-2, microtubule-associated protein-2; NCAM, neural cell adhesion molecule; PBS, phosphate-buffered saline.

abnormalities observed in infants with fetal alcohol related disorders.

L1, a transmembrane glycoprotein, is a member of the immunoglobulin superfamily of cell adhesion molecules (Moos *et al.* 1988). L1 is expressed on axonal shafts and growth cones of developing neurons (Craig *et al.* 1995; Kamiguchi and Lemmon 1998), and has an active role in axonal growth and guidance (Lagenaur and Lemmon 1987; Cohen *et al.* 1997). L1 binds in trans to itself, or to integrins (Yip *et al.* 1998) on adjacent axons. Cerebellar granule neuron (CGN) from L1 knock out mice completely lose their ability to extend neurites on L1, indicating the predominance of the L1 to L1 homophilic interaction (Fransen *et al.* 1998).

The gene for L1 is highly conserved among species and is comprised of 28 exons, of which exons 2 and 27 are alternatively spliced (Miura *et al.* 1991). Neural cells express an isoform of L1 containing the alternatively spliced exons, whereas non-neuronal cells such as Schwann cells do not (Takeda *et al.* 1996). The alternatively spliced exon 27 encodes for the amino acid sequence RSLE (Arg-Ser-Leu-Glu) immediately following a tyrosine residue 1176 [Y(1176)] in the cytoplasmic domain. This sequence conforms to a tyrosine based sorting motif, Yxx ϕ , where Y signifies tyrosine, x stands for any amino acid, and ϕ represents an amino acid with a bulky hydrophobic side chain (Trowbridge *et al.* 1993). Among the important functions of the YRSLE sequence are the regulation of L1 cell surface expression by endocytosis and the sorting of L1 to the growth cone membrane (Kamiguchi and Lemmon 1998; Kamiguchi *et al.* 1998; Wisco *et al.* 2003). Phosphorylation of Y(1176) inhibits endocytosis of L1 by inhibiting binding to the μ 2 chain of AP-2 (Schaefer *et al.* 2002). Dorsal root ganglions (DRGs) grown on laminin express only constitutively phosphorylated Y1176. Homophilic binding of L1 or cross-linking of L1 causes dramatic and rapid dephosphorylation of Y1176, allowing endocytosis and ERK1/2 activation to occur (Schaefer *et al.* 2002). Following endocytosis, Y1176 is rephosphorylated by an activated pp60^{src} (Schaefer *et al.* 2002).

There are three additional tyrosines within the cytoplasmic domain of L1 (L1CD), Y1151, Y1211, and Y1229. Y1151 is critical for binding to ezrin-radixin-moesin (Cheng *et al.* 2005) and Y1211 is within the ankyrin binding domain (Davis and Bennett 1994). The third, Y1229, is involved in regulation of ankyrin binding (Garver *et al.* 1997). Dephosphorylation and phosphorylation of this tyrosine regulates ankyrin binding which is involved in the stationary behavior of L1 (Gil *et al.* 2003).

We hypothesize that ethanol inhibits L1-mediated neurite outgrowth by either inhibiting the tyrosine sorting signal and thereby disrupting L1 sorting to the growth cone, or by inhibiting downstream signaling events preceding ERK1/2 activation.

Methods

Antibodies and inhibitors

Rabbit polyclonal antibodies against chick NgCAM (8D9) and mouse monoclonal antibodies against chick NCAM (1A6) and the dephosphorylated Y1176 L1 (74-5H7) have been previously described (Schaefer *et al.* 2002). NgCAM is the chick homolog of L1 and will be referred to as L1 in this paper. Polyclonal goat antibodies to the L1CD (anti-L1CD) were obtained from Santa Cruz Biotechnology (Santa Cruz, CA, USA). Polyclonal antibodies to phospho-Src family (Tyr416), phospho-p44/42 MAPK (Thr202/Tyr204), and p44/42 MAPK as well as a monoclonal antibody to phosphotyrosine, PY100 were obtained from Cell Signaling (Beverly, MA, USA). The monoclonal antibody against bovine microtubule-associated protein-2 (MAP-2) was purchased from Roche pharmaceuticals (Indianapolis, IN, USA) and the monoclonal antibody to pp60^{src} from clone GD11 was from Upstate (Lake Placid, NY, USA). Goat anti-mouse IgG (H + L), goat anti-rabbit IgG (H + L), fluorescein (FITC) conjugated affinity purified goat anti-mouse IgG (H + L) chain, rhodamine red X conjugated goat anti-rabbit IgG (H + L) chain, horseradish peroxidase (HRP)-conjugated goat anti-mouse IgG (H + L) and HRP-conjugated goat anti-Rabbit IgG (H + L) secondary antibodies were obtained from Jackson Immuno-Research Laboratories (West Grove, PA, USA). Alexa Fluor 633 dye conjugated donkey anti-goat and Alexa Fluor 488 dye conjugated goat anti-mouse were obtained from Molecular Probes (Eugene, OR, USA). Monoclonal anti- β tubulin III and the Texas red conjugated secondary antibody raised in goat against mouse IgG was from Sigma (St Louis, MO, USA). PP2, a selective inhibitor of the Src family of protein tyrosine kinases was obtained from Calbiochem (San Diego, CA, USA). Sodium vanadate was from Fisher (Pittsburgh, PA, USA).

Mouse monoclonal antibody to rat L1 (ASCS4) was produced from a hybridoma cell line developed by P. H. Patterson and obtained from the Developmental Studies Hybridoma Bank (The University of Iowa) as previously described (Tang *et al.* 2006). Preparation of a chimeric protein consisting of the extracellular domain of L1 and the Fc domain of IgG (L1-Fc) has been previously described (Bearer *et al.* 1999; Tang *et al.* 2006).

Cell culture

Dorsal root ganglions were dissected from the lumbar region of embryonic day 9–10 chicks, stages 35–36 per the Hamilton and Hamburger system (Hamburger and Hamilton 1951). The DRGs were dissociated sequentially with 2.4 units/mL dispase II (Roche) and 10 units/mL Dnase (Roche) in Ca²⁺/Mg²⁺-free phosphate-buffered saline (PBS). The cells were then washed with 10% fetal bovine serum (FBS) in Dulbecco's modified Eagle's medium (DMEM) (Gibco, Rockville, MD, USA) and centrifuged. The cell layer was added to an uncoated tissue culture dish containing growth media consisting of DMEM 10% FBS with 100 ng/mL mouse β nerve growth factor (Austral Biologicals, San Ramon, CA, USA). After an hour, the cell culture dish was agitated and the growth media with the detached cells in suspension was replated onto glass slides that were prepared as described in the next section. Cell cultures were maintained for 16–20 h in a 37°C humidified 90% air, 10% CO₂ incubator.

Rat post-natal day 6 CGN were prepared and plated on poly-L-lysine coated tissue culture dishes in DMEM, 10% FBS containing

20 mM HEPES, pH 7.4 and penicillin/streptomycin as previously described (Tang *et al.* 2006).

Glass slides were coated with either poly-L-lysine, protein A, L1-Fc or laminin

Poly-L-lysine: To prepare slides for DRGs, 500 μ L 0.1% poly-L-lysine solution (Sigma) was added to each chamber of a four chamber glass slide (Lab Tek, Naperville, IL, USA) for 30 min. The wells were then rinsed with Hank's balanced salt solution (HBSS) (Sigma) and allowed to air dry. **Protein A (Sigma):** For L1-Fc experiments, 80 μ L of protein A (2 mg/mL in 0.1 M potassium phosphate, pH 7.4) was added for 1 h at 37°C.

A chimeric protein consisting of the extracellular domain of L1 and the Fc domain of IgG: 7.3 μ g of L1-Fc eluted from protein A columns (Tang *et al.* 2006) was diluted into 50 μ L PBS 1% bovine serum albumin (BSA) and incubated for 1 h at 37°C to achieve 1.2 μ g/cm² L1-Fc per well. Slides prepared for experiments with permeabilized cells were plated with 3.5 μ g of L1-Fc in 50 μ L of PBS 1% BSA to achieve 0.6 μ g/cm² L1-Fc per well.

Laminin: Slides were treated with laminin (100 μ g/mL (Sigma) in Ca²⁺, Mg²⁺ free PBS) and incubated overnight at 37°C. Both L1-Fc and laminin coated slides were rinsed with HBSS, and blocked with 10% horse serum (Gibco) in 0.1 M potassium phosphate, pH 7.4, 0.05% sodium azide.

Ethanol exposure of DRG cultures

Immediately after transfer of the DRGs in growth media into prepared slide chambers, an equal volume of growth media containing 200 mM ethanol was added, for a final concentration of 100 mM ethanol, to the ethanol exposed DRG slides. Control slides had an equal volume of growth media without ethanol added. The slide chambers were covered and wrapped with parafilm. The ethanol containing slides were placed in a dedicated 37°C 10% CO₂ incubator with 100 mM ethanol in the water pan. We have previously shown that ethanol concentrations in the media are constant under these conditions (Bearer *et al.* 1999). Prior to fixation or antibody application, the growth media was removed and stored at 4°C for later determination of ethanol concentration by spectrophotometry (Cary 3E UV-Visible Spectrophotometer) with an alcohol dehydrogenase diagnostic kit (Roche). There was no more than a 20% reduction in ethanol level over the course of the experiment.

Immunocytochemistry of permeabilized DRGs

The cells were fixed and permeabilized for 15 min in Bouin's solution (1.2% picric acid, 37% formaldehyde), followed by repeated washes with potassium phosphate 0.1 M, pH 7.4, 0.05% azide. The slides were then incubated with blocking solution (10% horse serum in potassium phosphate 0.1 M, pH 7.4, 0.05% azide) for 1 h at 37°C, rinsed, and kept at 4°C overnight with primary antibodies to NCAM (1A6) 1 : 500 and L1 (8D9) 1 : 500 diluted in blocking solution. The slides were rinsed extensively with potassium phosphate buffer, before labeling with the secondary antibodies. Antibodies to L1 were identified with Rhodamine Red-X conjugated goat anti-rabbit and antibodies to NCAM were identified with FITC conjugated goat anti-mouse diluted 1 : 200 in blocking solution. The secondary antibodies were incubated at 37°C for 2 h, followed by repeated rinses. The slides were mounted with Slow

Fade Light (Molecular Probes) and viewed using a Zeiss LSM 410 Confocal laser scan microscope (Zeiss, Thornwood, NY, USA) with an oil immersion 100x objective.

Antibody to MAP-2 was used at 1 : 600 dilution in blocking solution and labeled with Texas Red goat anti-mouse secondary at 1 : 500 in blocking solution. Images were captured on a spot digital camera attached to a Nikon Optiphot-2 fluorescence microscope (Nikon, Melville, NY, USA).

Immunocytochemistry of CGN

Cerebellar granule neuron were placed on glass coverslips coated with L1-Fc. 25 mM ethanol was added to treated cells and cells were incubated overnight. Slide fixation was accomplished through the addition of 4% paraformaldehyde for 20 min followed by repeated washes with PBS. The slides were then incubated with blocking solution (3% BSA and 0.2% Triton X-100 in PBS, 0.05% azide) for 1 h at 37°C or kept at 4°C overnight. Primary antibodies to beta tubulin 1 : 1000 and L1CD 1 : 500 were diluted in blocking solution then incubated for 2 h at 37°C. The slides were rinsed extensively with PBS before labeling with the secondary antibodies. Antibodies to L1 were identified with Alexa Fluor 633 dye conjugated donkey anti-goat antibodies and antibodies to beta tubulin were identified with Alexa Fluor 488 dye conjugated goat anti-mouse antibodies diluted 1 : 200 in blocking solution. The secondary antibodies were incubated at 37°C for 1 h, followed by repeated rinses. The slides were mounted with Vectashield (Vector H-1200, Burlingame, CA, USA) containing 4,6-diamidino-2-phenylindole and viewed using a Zeiss LSM 410 Confocal laser scan microscope with an oil immersion 63x objective.

Immunocytochemistry of non-permeabilized DRGs

Slides with DRGs were placed on ice. The growth medium was carefully removed, and new ice-cold growth media containing primary antibodies to L1 (1 : 100) and NCAM (1 : 100) was carefully added to the DRG wells. The primary antibodies were incubated for 30 min, followed by three washes with ice cold growth media. The DRG cell cultures were kept at 4°C from the addition of the primary antibodies until fixation to prevent internalization of labeled cell surface adhesion molecules. Slide fixation was accomplished through the addition of 4% paraformaldehyde for 15 min. Rhodamine Red-X conjugated goat anti-rabbit (1 : 50 in blocking solution) secondary antibody to visualize L1 and FITC conjugated goat anti-mouse (1 : 50 in blocking solution) secondary antibody to visualize NCAM were added for 2 h at 37°C. In experiments designed to ascertain cell membrane integrity, mouse anti-MAP-2 (1 : 600 in growth media) primary antibody was labeled with Texas red conjugated goat anti-mouse (1 : 500 in blocking solution) and viewed with a Nikon Optiphot-2 fluorescent microscope.

Imaging analysis and growth cone selection

A slide prepared under identical conditions to the experimental slides, but known to have had no exposure to ethanol was used as a standard for determining the optimal confocal contrast and brightness settings. The microscope parameters were not altered while obtaining images of the ethanol and control slides. The individual selecting the growth cones for this study was blinded to the ethanol exposure status of the slide until the completion of data

collection. A growth cone was included in the study if it met the following criteria: extension of at least 50 μm from the cell body, characteristic morphologic structure, and no contact with another neurite (Lagenaur and Lemmon 1987). The slides were scanned using the fluorescein channel which showed NCAM staining. Growth cones were selected sequentially, starting at the upper left corner of each chamber. L1 was considered present at the growth cone if the neurite outline could be clearly delineated on the rhodamine 568 λ channel for which the L1 antibody was immunologically tagged. L1 presence in growth cones was analyzed by chi square. Statistical analysis was performed using Systat software v3.01 (Chicago, IL, USA).

L1 clustering on cerebellar granule cells

Growth medium was removed from CGN cultures and replaced with serum-free medium (DMEM, 20 mM HEPES, penicillin/streptomycin) for 2 h prior to L1 clustering; 25 mM ethanol was added to appropriate dishes 1 h prior to clustering. To form cross-linked ASCS4 antibody complexes, purified ASCS4 was mixed with goat anti-mouse IgG (H + L) (1 : 2.5 g/g) for 1 h at 4°C and then added to CGN such that the final concentration was 30 $\mu\text{g}/\text{mL}$ of media. Mouse IgG 30 $\mu\text{g}/\text{mL}$ final concentration was used as control as previously described (Schmid *et al.* 2000; Tang *et al.* 2006). At the indicated times, the tissue culture dishes were placed on ice, the media was removed, and the cells were washed with ice-cold HBSS. All procedures were at 4°C.

Immunoblotting and immunoprecipitation

Cell extracts were made by incubating cells in lysis buffer for 30 min. and then centrifuging the extract at maximum speed in a Beckman Superspeed Centrifuge for 10 min at 4°C to remove particulate material. Lysis buffer consisted of: 20 mM Tris, pH 7.4, 150 mM NaCl, 1% Triton X-100, 1 mM EDTA, 10% glycerol, 10 mM Na-vanadate, 10 mM NaF, 2 mM aprotinin, 0.1 mM phenylmethylsulfonyl fluoride, 1 μM leupeptin, 1 $\mu\text{g}/\text{mL}$ pepstatin, 10 $\mu\text{g}/\text{mL}$ turkey trypsin inhibitor, phosphatase inhibitor cocktail I (Sigma), and phosphate inhibitor cocktail II (Sigma).

For immunoprecipitation experiments with L1-CD or Src, the cell extract supernatants were transferred to clean microfuge tubes and pre-cleared with 1 μg rabbit IgG or mouse IgG for 1 h, then with 30 μL Protein A/G-agarose for 1 h, followed by low speed centrifugation. Supernatants were collected, and 2 μg of antibody was added. After 1 h incubation, 30 μL of protein A/G-agarose was added and lysates were incubated overnight. The tubes were centrifuged in a Beckman Superspeed microfuge at 1000 g for 4 min.

For Western analysis, proteins were precipitated from cell extract supernatants with methanol-chloroform and dried. Precipitants or immunoprecipitants were washed with lysis buffer, and boiled for 5 min in sodium dodecyl sulfate–polyacrylamide gel electrophoresis sample buffer. The samples were separated by sodium dodecyl sulfate–polyacrylamide gel electrophoresis (12% gel), transferred to a polyvinylidene fluoride membrane. The membrane was blocked in Tris-buffered saline containing 2% BSA and 0.1% Tween 20. The membrane was incubated with primary antibodies (74-5H7, phospho-Src (Tyr416) [phospho-src family (Tyr416) antibody], PY100 or phospho-p44/42 MAPK (Thr202/Tyr204) (pERK1/2) probed with either HRP-goat anti-mouse IgG or HRP-goat anti-rabbit IgG, and reactive protein bands were visualized using

enhanced chemiluminescence exposure of x-ray film. Blots were stripped and reprobed with antibodies to either the L1 cytoplasmic domain (L1CD) or p44/p42 MAPK (Total ERK1/2) followed by HRP-conjugated goat anti-rabbit IgG antibodies or anti-pp60^{src} followed by HRP-conjugated goat anti-mouse IgG antibodies. Blots were analyzed in a semiquantitative manner using Kodak (Rochester, NY, USA) 1D imaging software to measure the density of bands on the x-ray film. The 74-5H7 and PY100 band densities were normalized for the band densities of L1CD protein, band densities of pERK1/2 were normalized for the band densities of total ERK, and phospho-src family (Tyr416) antibody band densities were normalized to total pp60^{src} for all quantitative analyses. Relative densitometric units were calculated by calculating the ratio of the normalized band densities to that of the control.

Results

The total L1 present at the growth cone is not changed by the presence of ethanol

A target ethanol concentration of 100 mM was chosen as it approaches the maximum concentration of ethanol realistically achieved *in vivo* before lethal toxicity is likely to occur. Individuals who have developed a chronic tolerance to ethanol, however, may have blood ethanol levels as high as 245–300 mM (Deitrich and Harris 1996). An *in vitro* ethanol level of 100 mM does not significantly decrease DRG survival but does negatively impact neurite outgrowth (Bradley *et al.* 1995). Prior work in our lab has shown a half maximal inhibitory effect at 400 mM ethanol on laminin mediated cerebellar neurite outgrowth and a half maximal inhibitory effect from 3 to 5 mM ethanol for L1-Fc mediated cerebellar neurite outgrowth (Bearer *et al.* 1999). Thus, if the underlying effect of ethanol was to prevent L1 sorting to the growth cone, this specific effect would be visible at 100 mM.

To determine if ethanol disrupts intracellular transport of L1 from the cell body to the growth cone, we utilized two cell types: (i) DRGs because of their large and easily visible growth cones, and previously published results showing neurite outgrowth inhibition at 100 mM ethanol (Bradley *et al.* 1995) and failure of sorting to the growth cone when the tyrosine sorting signal was disrupted (Kamiguchi and Lemmon 1998); and (ii) CGN because of our previous results showing the inhibition of L1-mediated neurite outgrowth in the presence of ethanol (Bearer *et al.* 1999). Permeabilized DRGs were labeled with a rabbit anti-L1 antibody. L1 distribution was first examined in DRGs propagated on laminin substrate. Neurites growing on the extracellular matrix protein laminin depend upon integrin-mediated signaling for neurite extension (Drazba and Lemmon 1990). Neurites extending upon laminin were highly fasciculated and exhibited a characteristic growth cone morphology (Burden-Gulley *et al.* 1995; Nakai and Kamiguchi 2002) of small lamellipodial domains from which long filopodia

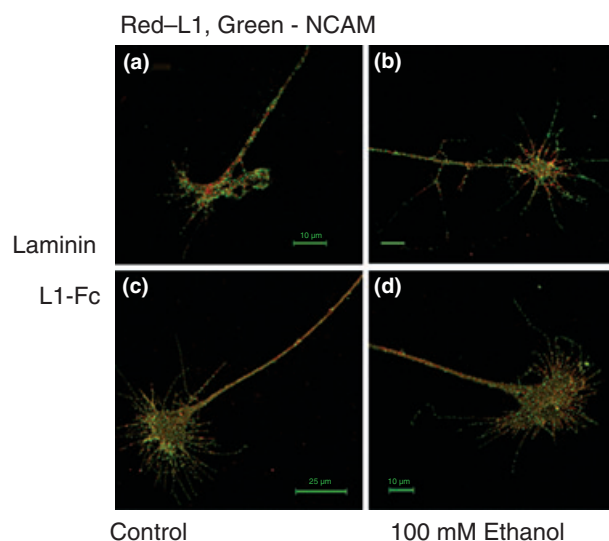


Fig. 1 Exposure to ethanol does not affect growth cone distribution of total L1. (a and b) Representative DRG growth cones adherent to laminin substrate. Confocal images show the total L1 present at the growth cone in red and the total NCAM in green. L1 distribution in the no ethanol control growth cone (a) is similar to the L1 distribution found in the growth cone exposed to 100 mM ethanol (b). (c and d) DRG growth cones adherent to L1-Fc substrate exhibit a different morphology compared to those propagated on laminin. Despite this difference, the distribution of total L1 is the same for the no ethanol control growth cone (c) and the 100 mM exposed growth cone (d).

extend. L1 was similarly distributed within the growth cone lamellipodia and filopodia in both the no ethanol control group (Fig. 1a) and the ethanol group (Fig. 1b). L1 was present in all 111 control and 152 ethanol exposed growth cones. The results pooled from 11 separate experiments are summarized in Table 1.

Next, the distribution of L1 on growth cones of DRGs cultured on L1-Fc substrate was examined. These neurites extended in a defasciculated pattern and growth cones exhibited broader lamellipodia and shorter filopodia com-

Table 1 Ethanol does not alter the distribution of L1 at the growth cone

Experiment type	Control		Ethanol	
	Cells counted	Cells with L1 in growth cone (%)	Cells counted	Cells with L1 in growth cone (%)
Total L1/laminin substrate ($n = 11$)	111	111 (100%)	152	152 (100%)
Total L1/L1-Fc substrate ($n = 3$)	91	90 (98.9%)	97	96 (99.0%)
Extracellular L1/L1-Fc substrate ($n = 3$)	85	85 (100%)	94	94 (100%)

L1, cell adhesion molecule; L1-Fc, a chimeric protein consisting of the extracellular domain of L1 and the Fc domain of IgG.

pared to DRG grown on laminin, as previously reported (Burden-Gulley *et al.* 1995; Nakai and Kamiguchi 2002). Once again, L1 was distributed throughout all areas of nearly all growth cones in both the control (Fig. 1c) and ethanol exposed groups (Fig. 1d; Table 1).

To confirm these results in CGN, CGN were plated on L1-Fc, and exposed to 25 mM ethanol for 1 h. Growing tips of neurites were identified by anti- β tubulin. L1 was present in all tips of all neurites examined (Fig. 2).

Although these results show that ethanol did not disrupt the transportation of L1 to the growth cone, it is unclear whether ethanol disrupted the insertion of L1 into the cell membrane. Proper membrane insertion is critical for L1-mediated growth cone motility which involves endocytosis and recycling of L1 back to the leading edge of the growth cone (Kamiguchi and Lemmon 2000).

Applying primary antibody to living cells allows localization of cell surface antigens

To examine the effect of ethanol on the proper insertion of L1 into plasma membranes, antibodies were applied to living cells to determine whether the extracellular domain of L1 was present on the surface of growth cones.

To differentiate between an external or internal location of an antigen, primary antibodies were applied to living cells prior to fixation. The cell cultures were maintained at 4°C over a 30 min incubation period to suspend cellular activity thereby preventing internalization of cell surface molecules. Membrane integrity was tested using antibodies against the intracellular protein MAP-2. If the cell membrane is not disrupted, MAP-2 will not be visualized by immunohistochemistry.

Control DRG cell cultures were fixed with 4% paraformaldehyde for 15 min, followed by application of mouse anti-MAP-2. The fixation process caused enough disruption of the cell membrane to allow binding of the primary antibody to MAP-2 antigen, as visualized after the application of Texas red goat anti-mouse (Fig. 3a). The DRG cell cultures undergoing primary antibody application while still alive were cooled to 4°C, incubated with primary antibody, washed repeatedly with cold growth media, fixed with 4% paraformaldehyde, and finally labeled with Texas red goat anti-mouse secondary antibody. In contrast to the DRG cultures that were fixed prior to antibody application, anti-MAP-2 could not bind to internal antigen when applied to living DRG cells. As MAP-2 is solely intracellular, it was not visualized by this method (Fig. 3b).

The L1 present at the growth cone surface is not changed by the presence of ethanol

We examined DRG cultures grown on L1-Fc substrate and labeled at 4°C with rabbit anti-L1 (8D9). We found that L1 was present on the surface of growth cones. DRGs were grown on 0.6 $\mu\text{g}/\text{cm}^2$ L1-Fc to minimize background

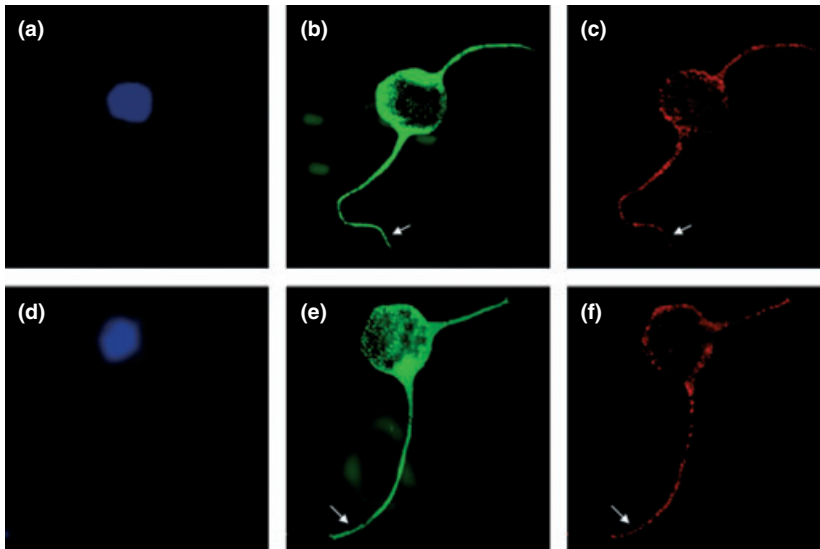


Fig. 2 Exposure to ethanol does not affect growth cone distribution of total L1 in CGN. A representative cell from ethanol exposed and control experiments is shown. Cell bodies were identified by DAPI (a and d). The immunocytochemical distribution of beta tubulin (b and e) and L1 (red, c and f) was examined using confocal images of CGN cultured on L1-Fc overnight. No difference between L1 distribution along the tips of the neuritis (arrows) of CGN exposed to 25 mM ethanol (a–c) and that of control (d–f) can be detected.

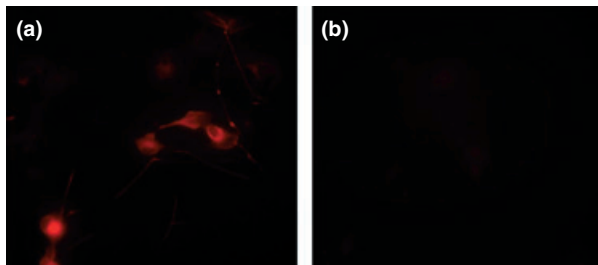


Fig. 3 Application of antibody prior to cell fixation selectively targets extracellular antigen as determined by intracellular MAP-2 detection. Slides of DRG cells were prepared by the standard immunocytochemistry method of fixation with 4% paraformaldehyde followed by antibody application. (a) Intracellular MAP-2 is present in the DRG cell bodies and proximal axons. Fixation caused enough disruption of the cell membrane to enable antibody attachment to MAP-2. (b) The application of antibody to cooled DRG cells before fixation labels only proteins with extracellular domains. Because antibody-antigen binding occurred before fixation perturbed cell membrane integrity, intracellular MAP-2 is not labeled and cannot be visualized. Arrows indicate cell bodies.

interference. The distribution pattern of cell surface L1 was similar in both ethanol and control samples (Table 1). Immunofluorescence was prominent at the P domain of the growth cone, or leading edge, where L1 is active in neuronal guidance (Kamiguchi and Lemmon 1998; Nakai and Kamiguchi 2002). L1 was observed at the growth cone in the control cells as well as in the ethanol exposed cells (Fig. 4a and b).

Ethanol inhibits the dephosphorylation of the YRSL domain of L1

Previously, it has been shown that the targeting of L1 to the plasma membrane is regulated by the dephosphorylation of

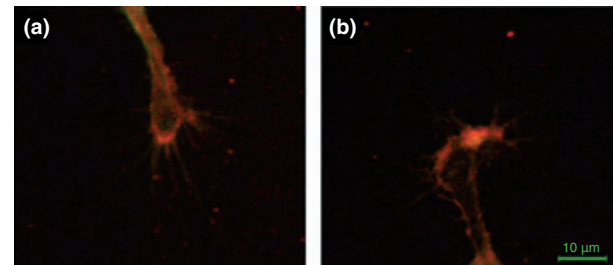


Fig. 4 L1 is present at the cell surface of DRG growth cones propagated on L1-Fc substrate. Chick L1 is visualized using antibody specific for chick L1. Cell surface L1 was prominent at the leading edge of the growth cone during L1-mediated neurite outgrowth. There was no difference in surface L1 distribution between the control growth cones (a) and the 100 mM ethanol exposed growth cones (b).

the YRSL domain of L1, which can be identified by the monoclonal antibody, 74-5H7 (Schaefer *et al.* 2002). In DRGs sparsely cultured on laminin, no 74-5H7 immunoreactivity was observed. However, following L1 clustering on the cell surface using a polyclonal anti-L1 antibody, a rapid appearance of 74-5H7 immunoreactivity was observed (Schaefer *et al.* 2002). These results indicate that the tyrosine of the YRSL is constitutively phosphorylated for axonal sorting to the plasma membrane as no 74-5H7 immunoreactivity is seen prior to L1 clustering. However, following L1 activation on the cell surface, a dephosphorylation of Y1176 occurs.

To test whether ethanol interferes with this dephosphorylation, CGN were grown on poly-L-lysine overnight in serum containing media, then serum starved for 2 h prior to clustering of cell surface L1. In some cases, 25 mM ethanol was added for 1 h prior to L1 clustering. As can be seen in

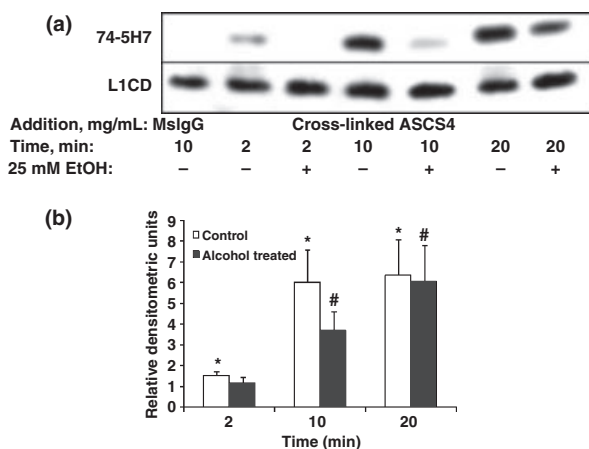


Fig. 5 Y1176 is dephosphorylated by addition of cross-linked ASCS4 and is inhibited by ethanol. (a) Serum starved CGN were treated with 25 mM ethanol for 1 h, then either mouse IgG (MslgG), or cross-linked ASCS4 was added for 2, 10, or 20 min. Dephosphorylation of Y1176 was assayed by western blot analysis. Western blots showed that addition of cross-linked ASCS4 significantly increased dephosphorylation of Y1176 (74-5H7) at 2, 10, and 20 min in the absence of ethanol (no alcohol). Significant inhibition of ASCS4 mediated Y1176 dephosphorylation occurred in ethanol pre-treated cells (one of four representative blots shown) at 10 and 20 min (alcohol treated). Detection of L1 by polyclonal antibody to the cytoplasmic domain of L1 (L1CD) is used as loading control. (b) Dephosphorylation of Y1176 is significantly increased at 2, 10, and 20 min following addition of cross-linked ASCS4. One hour pre-treatment with 25 mM ethanol significantly reduces dephosphorylation of Y1176 at 10 and 20 min, although it remains significantly increased over mouse MslgG at 10 and 20 min (alcohol treated). Densitometric quantification of Y1176 dephosphorylation corrected for total L1 shown in (a) is plotted as relative densitometric units relative to the MslgG control. The values of four separate experiments are shown. The bar indicates the mean of the values \pm SE. The single asterisk (*) indicates a statistically significant increase in dephosphorylated Y1176 following addition of cross-linked ASCS4 (no alcohol) versus MslgG ($p < 0.05$, paired t -test). The number sign (#) indicates a statistically significant decrease in Y1176 dephosphorylation following alcohol pre-treatment (alcohol treated) ($p < 0.05$, paired t -test).

Fig. 5(a and b), in the absence of L1 clustering, CGN had minimal 74-5H7 immunoreactivity (mouse IgG control), similar to that reported for DRGs (Schaefer *et al.* 2002). However, following addition of cross-linked ASCS4 to induce clustering of L1, 74-5H7 immunoreactivity was initially observed at 2 min with a sustained peak at 10–20 min, a time course similar to that seen in DRGs (Schaefer *et al.* 2002). In the cells pre-treated for 1 h with 25 mM ethanol, a reduction in 74-5H7 immunoreactivity was observed at both 10 and 20 min, but more marked at 10 min (Fig. 5a and b). At 20 min, the difference between 74-5H7 immunoreactivity in control and ethanol exposed

cells was less, indicating that ethanol's effect was primarily a delay in the dephosphorylation of Y1176.

Ethanol inhibits L1 tyrosine phosphorylation

The phosphorylation/dephosphorylation of tyrosine Y1229 of L1 has been shown to regulate binding of L1 to ankyrin (Garver *et al.* 1997). Regulation of L1 binding to ezrin-radixin-moesin and ankyrin may be regulated by phosphorylation/dephosphorylation of tyrosines 1151 and 1211, respectively. To determine whether ethanol influences tyrosine phosphorylation following clustering of L1, we added cross-linked ASCS4 to serum starved CGN, and measured tyrosine phosphorylation by using anti-phosphotyrosine monoclonal antibodies on immunoblots of immunoprecipitated L1. Tyrosine phosphorylation was quantified by stripping blots and reprobing for total L1 using anti-L1CD. Values were normalized to controls. The results in Fig. 6 show that the addition of cross-linked ASCS4 significantly increased tyrosine phosphorylation of L1, and that the addition of 25 mM ethanol 1 h prior to addition of ASCS4 blocked this response. Interestingly, the tyrosine phosphorylation appears to occur prior to the dephosphorylation of Y1176. It also appears that the anti-PY antibody does not recognize Y1176 as in controls, Y1176 is constitutively phosphorylated (i.e. is not recognized by 74-5H7, see Fig. 5) but there is little phosphotyrosine detected by anti-PY in control cells (see Fig. 6).

Ethanol inhibits L1-mediated activation of pp60^{src}

pp60^{src} has been shown to be activated following the clustering of L1 (Schmid *et al.* 2000) which leads to rephosphorylation of Y1176 (Schmid *et al.* 2000). To determine whether ethanol influences pp60^{src} activation following clustering of L1, we added cross-linked ASCS4 to serum starved CGN, and measured activated pp60^{src} by using polyclonal antibodies to phospho-src (Tyr416) on immunoblots of immunoprecipitated pp60^{src}. Activated pp60^{src} was quantified by stripping blots and reprobing for total pp60^{src}. Values were normalized to controls. Results in Fig. 7 show that the addition of cross-linked ASCS4 significantly increased tyrosine 416 phosphorylation of pp60^{src}, and that the addition of 25 mM ethanol 1 h prior to addition of ASCS4 blocked this response. The activation of pp60^{src}, like L1 tyrosine phosphorylation, appears to occur prior to the dephosphorylation of Y1176, suggesting that pp60^{src} is activated prior to the endocytosis of L1. These findings are consistent with those previously reported (Schmid *et al.* 2000).

Order of signaling cascade downstream from L1

We have now shown that ethanol inhibits L1-mediated dephosphorylation of Y1176, tyrosine phosphorylation of L1 and activation of both pp60^{src} and ERK1/2 (Tang *et al.* 2006). In order to delineate what was a direct effect of

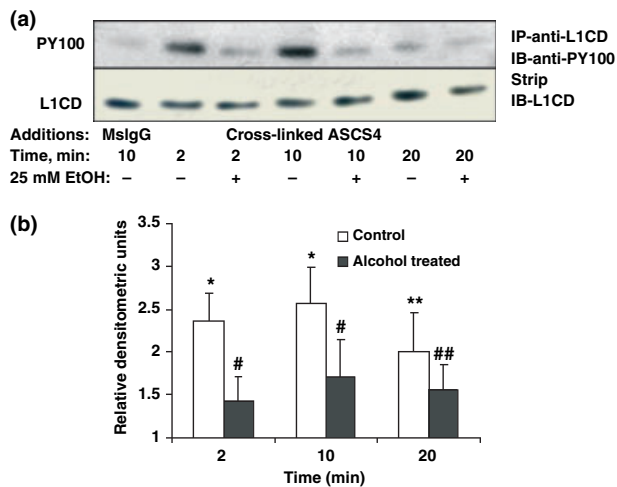


Fig. 6 Tyrosine phosphorylation is increased by addition of cross-linked ASCS4 and is blocked by ethanol. (a) Serum starved CGN were treated with 25 mM ethanol for 1 h, then cross-linked ASCS4 was added for 2, 10, or 20 min. Control cells were harvested 10 min after addition of mouse IgG (MslgG). Tyrosine phosphorylation was assayed by immunoprecipitation of L1 followed by western blot analysis for phosphotyrosine (PY100). Blots were stripped and re-probed with antibody to the cytoplasmic domain of L1 (L1CD) as a loading control. Western blots showed that addition of cross-linked ASCS4 significantly increased tyrosine phosphorylation at 2, 10, and 20 min in the absence of ethanol (no alcohol). No increase in tyrosine phosphorylation was seen in the presence of ethanol (alcohol treated). (b) Densitometric quantification of tyrosine phosphorylation corrected for total L1 shown in (a) is plotted as relative densitometric units relative to the MslgG control. The values of four separate experiments are shown. The bar indicates the mean of the values \pm SE. The single and double asterisks indicate statistically significant increase in tyrosine phosphorylation following addition of cross-linked ASCS4 versus the MslgG control (* p < 0.02; ** p < 0.05, paired t -test). The single and double number signs indicate statistically significant decreases in tyrosine phosphorylation following alcohol pre-treatment (alcohol treated) (# p < 0.005; ## p < 0.05, paired t -test). There was no significant difference in tyrosine phosphorylation at any time point from the MslgG control in the presence of ethanol (alcohol treated).

ethanol rather than a secondary effect, we sought to determine the order of these signaling events. The data presented in Figs 5–7 and our previous findings with ERK1/2 (Tang *et al.* 2006) suggest that pp60^{src} activation and tyrosine phosphorylation of L1 precede dephosphorylation of L1 and ERK1/2 activation. Using PP2 to selectively inhibit src kinases and sodium vanadate to inhibit phosphatases, L1 was activated by cross-linked ASCS4. The dephosphorylation of Y1176, tyrosine phosphorylation of L1, and the activation of pp60^{src} and ERK1/2 were measured. The results are shown in Fig. 8. Addition of dimethylsulfoxide (DMSO), the vehicle for

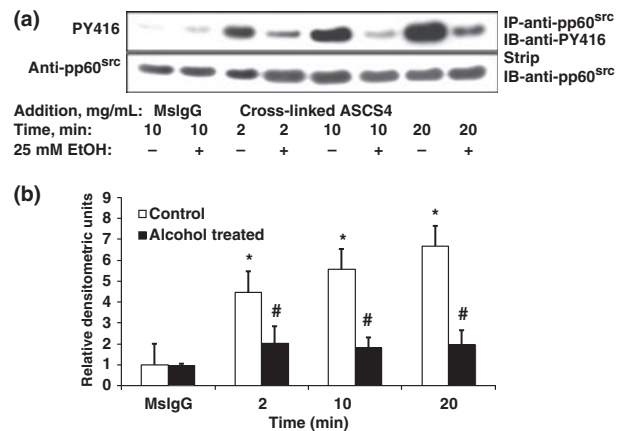


Fig. 7 pp60^{src} is activated by addition of cross-linked ASCS4 and is blocked by ethanol. (a) Serum starved CGN were treated with 25 mM ethanol for 1 h, then cross-linked ASCS4 was added for 2, 10, or 20 min. Control cells were harvested 10 min after addition of mouse IgG (MslgG). Activated pp60^{src} was assayed by immunoprecipitation of pp60^{src} followed by western blot analysis for phospho-Src family (Tyr416) (PY416). Blots were stripped and re-probed with anti-pp60^{src} as a loading control. Western blots showed that addition of cross-linked ASCS4 significantly increased activation of pp60^{src} at 2, 10, and 20 min in the absence of ethanol (no alcohol). No increase in activated pp60^{src} was seen in the presence of ethanol (alcohol treated). One of three representative blots shown. (b) Densitometric quantification of PY416 corrected for total pp60^{src} shown in (a) is plotted as relative densitometric units relative to the MslgG control. The values of three separate experiments are shown. The bar indicates the mean of the values \pm SE. The single asterisks indicate statistically significant increases in pp60^{src} tyrosine phosphorylation following addition of cross-linked ASCS4 versus MslgG control (* p < 0.05, paired t -test). The number signs indicate statistically significant decreases in pp60^{src} PY416 following alcohol pre-treatment (# p < 0.05, paired t -test). There was no significant difference between pp60^{src} tyrosine phosphorylation at any time point compared to the MslgG control in the presence of ethanol.

PP2, had no effect on any reaction. As expected, the addition of DMSO/PP2 and vanadate resulted in significant inhibition of activation of pp60^{src} and dephosphorylation of Y1176 respectively. Addition of DMSO/PP2 also inhibited the dephosphorylation of Y1176, tyrosine phosphorylation of L1, and activation of ERK1/2. In contrast, addition of vanadate had no effect on activation of pp60^{src}, tyrosine phosphorylation of L1, and activation of ERK1/2. However, lack of inhibition of tyrosine kinase activities in the presence of a phosphatase inhibitor is difficult to interpret as vanadate may increase phosphorylation by itself. These results are consistent with the activation of pp60^{src} as the proximal step in L1 downstream signaling. Hence, inhibition of the L1 activation of pp60^{src} by ethanol could account for the results presented here.

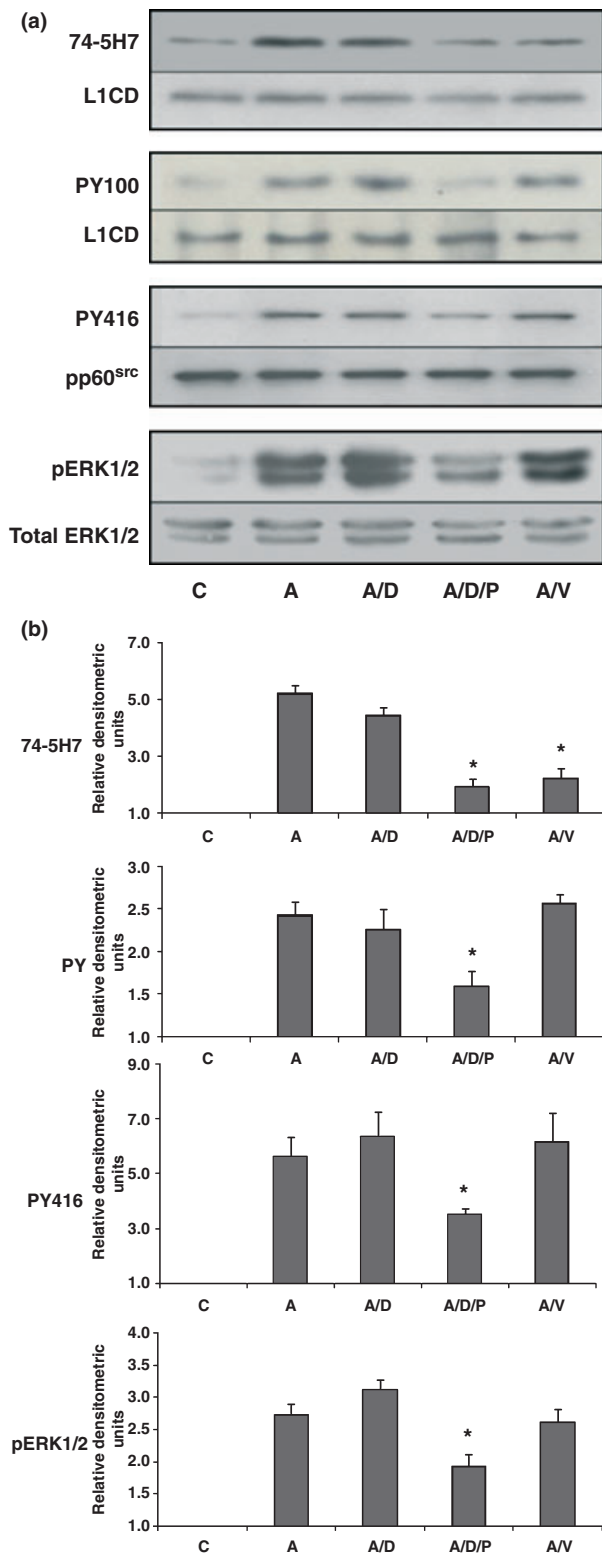


Fig. 8 pp60^{src} activation is the proximal step in downstream signaling of L1. (a) Serum starved CGN were activated with cross-linked ASCS4 for 10 min following a 1 h treatment with nothing (a only), dimethylsulfoxide (DMSO) (A/D), DMS with PP2 (A/D/P), or sodium vanadate (A/V). Control cells (Ctrl) were harvested 10 min after addition of mouse IgG (MslgG). Dephosphorylation of Y1176 (74-5H7), tyrosine phosphorylation of L1 (PY100) and activation of pp60^{src} (PY416) were assayed as described in Figs 5–7. The MAPK ERK1/2 was assayed by immunoblot of cell lysates with phospho-p44/42 MAPK (Thr202/Tyr204) (pERK1/2). Blots were stripped and reprobbed with p44/42 MAPK (total ERK1/2) as a loading control. One of three representative blots shown. (b) Densitometric quantification of immunoblots shown in (a) are plotted as relative densitometric units relative to the control. The values of three separate experiments are shown. The bar indicates the mean of the values \pm SE. The single asterisks indicate statistically significant decreases the ASCS4 alone control (a) (* $p < 0.05$, paired t -test).



Fig. 9 Diagram of proposed sequence of L1 signal transduction.

growth cone, or the insertion of L1 into the growth cone membrane; (ii) L1 in CGN is constitutively phosphorylated on the tyrosine of the YRSL sorting signal as observed in DRGs; (iii) clustering of L1 on the surface of CGN results in a dephosphorylation of Y1176 with a time course similar to that of DRGs; (iv) clustering of L1 increases L1 tyrosine phosphorylation and activation of pp60^{src}; (v) 25 mM ethanol dramatically reduces these signaling events; and (vi) pp60^{src} is proximal in the downstream signaling cascade of L1. These results are consistent with our previous findings that ethanol inhibits the phosphorylation of ERK1/2 induced by L1 clustering (Tang *et al.* 2006). Transfection with dominant negative src inhibits L1 endocytosis and L1-mediated activation of ERK1/2 (Schmid *et al.* 2000). L1-mediated activation of ERK1/2 (Schmid *et al.* 2000) and L1-mediated neurite outgrowth (Ignelzi *et al.* 1994) are also inhibited in cerebellar granule cells homozygous for src gene knockout. PP1, a src inhibitor, has been shown to inhibit L1 activation of ERK1/2 (Schaefer *et al.* 1999). If ethanol inhibits L1 activation of pp60^{src}, then dephosphorylation of the Y1176, endocytosis and MAPK activation would decrease. These effects should dramatically inhibit L1-mediated neurite outgrowth and produce the types of neurodevelopmental abnormalities observed in fetal alcohol syndrome. Our proposed sequence of events is shown in Fig. 9. We proposed that tyrosine phosphorylation of L1 follows pp60^{src} activation due to the early changes at 2 min in our immunoblots. Dephosphorylation occurs next with a slower onset from the immunoblots, and ERK1/2 activation is last based on reports that dephosphorylation of Y1176 is

Discussion

This study yielded several important new findings: (i) in DRGs, ethanol had no effect on either sorting of L1 to the

required for L1 endocytosis and ERK1/2 activation (Schaefer *et al.* 2002).

Neurite outgrowth on laminin was not inhibited by ethanol (Bearer *et al.* 1999). A disruption by ethanol of L1-mediated activation of pp60^{src} may be the underlying reason for the specificity of the ethanol effect on neurite outgrowth. CGN from wild type or src^{-/-} mice have the same neurite outgrowth when plated on laminin (Ignelzi *et al.* 1994) showing the independence from pp60^{src} of laminin mediated neurite outgrowth. These observations are consistent with the hypothesis that disruption by ethanol of pp60^{src} activation by L1 is the critical site of ethanol action.

The inhibition by ethanol of pp60^{src} may occur by several different mechanisms: (i) by an inhibition of pp60^{src} independent of L1, or (ii) by disrupting the protein-protein interactions necessary for L1 signaling to activate pp60^{src}.

Ethanol has been previously shown to prevent src activation leading to increased endocytosis of the NR2 subunit of the NMDA receptor in a hippocampal slice preparation (Suvarna *et al.* 2005). The inhibition was felt to be secondary to activation of H-Ras by ethanol. However, in a hippocampal slice, many signaling events could be occurring at baseline. Inhibition of any of these pathways may also reduce src activation. H-Ras is not involved in L1 signaling (Schmid *et al.* 2000) and ethanol treatment alone did not affect levels of activated pp60^{src} in our CGN preparation. Ethanol may act directly on the enzymes catalyzing tyrosine phosphorylation-dephosphorylation of tyrosine 416 and tyrosine 529 of src. Ethanol alters tyrosine phosphorylation in a number of systems examined including the NMDA receptor (Alvestad *et al.* 2003; Ferrani-Kile *et al.* 2003), the insulin receptor (Seiler *et al.* 2000), the insulin-like growth factor-1 receptor (Hallak *et al.* 2001), and both Cas and Cbl (Nishio and Suzuki 2002; Nishio *et al.* 2002). For the NMDA receptor, ethanol both increased the activity of tyrosine phosphatases as well as increased tyrosine kinases, whereas ethanol inhibited the tyrosine kinase activity of the insulin-like growth factor-1 receptor.

Second, ethanol may act by inhibiting the events between L1 activation and activation of pp60^{src} such as trafficking to a compartment containing both L1 and src. Lipid rafts may be one such compartment. Lipid rafts are platforms for bringing together signaling molecules. Recently, L1 has been found associated with lipid rafts (Nakai and Kamiguchi 2002). Localized perturbation of the lipid rafts in the P domain, but not the C domain of the growth cone reduced neurite outgrowth on an L1 substrate. It may be that ethanol inhibits L1 from trafficking through lipid rafts, and hence not interacting with the pp60^{src}, a known resident of lipid rafts (Encinas *et al.* 2004). Three papers have recently been published examining the effect of ethanol on the partitioning of specific proteins in lipid rafts. Ethanol blocked the lipopolysaccharide redistribution of CD14 to a lower density fraction of the lipid raft (Dai *et al.* 2005). Ethanol inhibited

the lipopolysaccharide-mediated redistribution of toll-like receptor 4 to the lipid raft, but had no effect on the peptidoglycan mediated redistribution of toll-like receptor 2 (Dolganuic *et al.* 2006). Insulin treatment of adipocytes from rats recruited cCbl and TC10 to lipid rafts. However, in adipocytes from rats chronically fed ethanol, insulin treatment did not translocate cCbl and TC10 to the lipid raft (Sebastian and Nagy 2005). L1-mediated neurite outgrowth may be dependent on protein-protein interactions in the lipid raft because recent data suggests that the L1CD may not be critical for this function (Cheng and Lemmon 2004).

Third, ethanol may inhibit the direct interaction of proteins such as that of receptors with scaffolding proteins. One recently reported example is that of Fyn kinase, a src family member, and the NMDA receptor. Fyn kinase is targeted to the NMDA receptor by the scaffolding protein receptor for activated C kinase 1. During acute exposure to ethanol, receptor for activated C kinase 1 dissociates from the Fyn kinase/NMDA receptor complex, facilitating tyrosine phosphorylation of the receptor (Yaka *et al.* 2003). In our system, ethanol may be disrupting the protein-protein interactions necessary to phosphorylate tyrosines in src.

Our results implicate that the major effect of ethanol on L1 is not on the sorting signal itself, but on its activation of pp60^{src}. Inhibition of pp60^{src} activation by L1 would inhibit subsequent L1 dephosphorylation, endocytosis, ERK activation, and, therefore, neurite outgrowth. These results suggest that the neurodevelopmental abnormalities observed in fetal alcohol syndrome could result from ethanol's effects on L1-mediated axon outgrowth.

Acknowledgements

We wish to thank H. Kamiguchi, M. Pendergast, and D. Major for their assistance in performing these studies. This work was supported by National Institutes of Health Grants AA-11839 and AA-016398 to C. F. Bearer and HD-039884 to V. Lemmon. C. F. Bearer holds the Cobey Professorship in Neonatology. V. Lemmon holds the Walter G. Ross Chair in Developmental Neuroscience at the Univ. of Miami.

References

- Alvestad R. M., Grosshans D. R., Coultrap S. J., Nakazawa T., Yamamoto T. and Browning M. D. (2003) Tyrosine dephosphorylation and ethanol inhibition of N-Methyl-D-aspartate receptor function. *J. Biol. Chem.* **278**, 11020–11025.
- Bearer C. F. (2001) Mechanisms of brain injury: L1 cell adhesion molecule as a target for ethanol-induced prenatal brain injury. *Semin. Pediatr. Neurol.* **8**, 100–107.
- Bearer C. F., Swick A. R., O'Riordan M. A. and Cheng G. (1999) Ethanol inhibits L1-mediated neurite outgrowth in postnatal rat cerebellar granule cells. *J. Biol. Chem.* **274**, 13264–13270.
- Bradley D. M., Paiva M., Tonjes L. A. and Heaton M. B. (1995) In vitro comparison of the effects of ethanol and acetaldehyde on dorsal root ganglion neurons. *Alcohol. Clin. Exp. Res.* **19**, 1345–1350.

- Burden-Gulley S. M., Payne H. R. and Lemmon V. (1995) Growth cones are actively influenced by substrate-bound adhesion molecules. *J. Neurosci.* **15**, 4370–4381.
- Charness M., Safran R. and Perides G. (1994) Ethanol inhibits neural cell-cell adhesion. *J. Biol. Chem.* **269**, 9304–9309.
- Cheng L. and Lemmon V. (2004) Pathological missense mutations of neural cell adhesion molecule L1 affect neurite outgrowth and branching on an L1 substrate. *Mol. Cell. Neurosci.* **27**, 522–530.
- Cheng L., Itoh K. and Lemmon V. (2005) L1-mediated branching is regulated by two ezrin-radixin-moesin (ERM)-binding sites, the RSLE region and a novel juxtamembrane ERM-binding region. *J. Neurosci.* **25**, 395–403.
- Cohen N. R., Taylor J. S. H., Scott L. B., Guillery R. W., Soriano P. and Furley A. J. W. (1997) Errors in corticospinal axon guidance in mice lacking the neural cell adhesion molecule L1. *Curr. Biol.* **8**, 26–33.
- Craig A. M., Wyborski R. J. and Banker G. (1995) Preferential addition of newly synthesized membrane protein at axonal growth cones. *Nature* **375**, 592–594.
- Dai Q., Zhang J. and Pruetz S. B. (2005) Ethanol alters cellular activation and CD14 partitioning in lipid rafts. *Biochem. Biophys. Res. Commun.* **332**, 37–42.
- Davis J. Q. and Bennett V. (1994) Ankyrin binding activity shared by the neurofascin/L1/NrCAM family of nervous system cell adhesion molecules. *J. Biol. Chem.* **269**, 27163–27166.
- Deitrich R. A. and Harris R. A. (1996) How much alcohol should I use in my experiments? *Alcohol. Clin. Exp. Res.* **20**, 1–2.
- Dolganic A., Bakis G., Kodys K., Mandrekar P. and Szabo G. (2006) Acute ethanol treatment modulates Toll-like receptor-4 association with lipid rafts. *Alcohol. Clin. Exp. Res.* **30**, 76–85.
- Drazba J. and Lemmon V. (1990) The role of cell adhesion molecules in neurite outgrowth on Muller cells. *Dev. Biol.* **138**, 82–93.
- Encinas M., Crowder R. J., Milbrandt J. and Johnson E. M. Jr (2004) Tyrosine 981, a novel ret autophosphorylation site, binds c-Src to mediate neuronal survival. *J. Biol. Chem.* **279**, 18262–18269.
- Ferrani-Kile K., Randall P. K. and Leslie S. W. (2003) Acute ethanol affects phosphorylation state of the NMDA receptor complex: implication of tyrosine phosphatases and protein kinase A. *Brain Res. Mol. Brain Res.* **115**, 78–86.
- Fransen E., D'Hooge R., Van Camp G. *et al.* (1998) L1 knockout mice show dilated ventricles, vermis hypoplasia and impaired exploration patterns. *Hum. Mol. Genet.* **7**, 999–1009.
- Garver T. D., Ren Q., Tuvia S. and Bennett V. (1997) Tyrosine phosphorylation at a site highly conserved in the L1 family of cell adhesion molecules abolishes ankyrin binding and increases lateral mobility of neurofascin. *J. Cell Biol.* **137**, 703–714.
- Gil O. D., Sakurai T., Bradley A. E., Fink M. Y., Cassella M. R., Kuo J. A. and Felsenfeld D. P. (2003) Ankyrin binding mediates L1CAM interactions with static components of the cytoskeleton and inhibits retrograde movement of L1CAM on the cell surface. *J. Cell Biol.* **162**, 719–730.
- Hallak H., Seiler A. E., Green J. S., Henderson A., Ross B. N. and Rubin R. (2001) Inhibition of insulin-like growth factor-I signaling by ethanol in neuronal cells. *Alcohol. Clin. Exp. Res.* **25**, 1058–1064.
- Hamburger V. and Hamilton H. L. (1951) A series of normal stages in the development of the chick embryo. *J. Morphol.* **88**, 49–92.
- Ignelzi M., Miller D., Soriano P. and Maness P. (1994) Impaired neurite outgrowth of src-minus cerebellar neurons on the cell adhesion molecule L1. *Neuron* **12**, 873–884.
- Kamiguchi H. and Lemmon V. (1998) A neuronal form of the cell adhesion molecule L1 contains a tyrosine-based signal required for sorting to the axonal growth cone. *J. Neurosci.* **18**, 3749–3756.
- Kamiguchi H. and Lemmon V. (2000) Recycling of the cell adhesion molecule L1 in axonal growth cones. *J. Neurosci.* **20**, 3676–3686.
- Kamiguchi H., Long K. E., Pendergast M., Schaefer A. W., Rapoport I., Kirchhausen T. and Lemmon V. (1998) The neural cell adhesion molecule L1 interacts with the AP-2 adaptor and is endocytosed via the clathrin-mediated pathway. *J. Neurosci.* **18**, 5311–5321.
- Lagenaur C. and Lemmon V. (1987) An L1-like molecule, the 8D9 antigen, is a potent substrate for neurite extension. *Proc. Natl Acad. Sci. USA* **84**, 7753–7757.
- Miura M., Kobayashi M., Asou H. and Uyemura K. (1991) Molecular cloning of cDNA encoding the rat neural cell adhesion molecule L1. Two L1 isoforms in the cytoplasmic region are produced by differential splicing. *FEBS Lett.* **289**, 91–95.
- Moos M., Tacke R., Schere H., Teplow D., Fruh K. and Schachner M. (1988) Neural adhesion molecule L1 as a member of the immunoglobulin superfamily with binding domains similar to fibronectin. *Nature* **334**, 701–703.
- Nakai Y. and Kamiguchi H. (2002) Migration of nerve growth cones requires detergent-resistant membranes in a spatially defined and substrate-dependent manner. *J. Cell Biol.* **159**, 1097–1108.
- Nishio H. and Suzuki K. (2002) Ethanol-induced Cas tyrosine phosphorylation and Fyn kinase activation in rat brain. *Alcohol. Clin. Exp. Res.* **26** (Suppl. 8), 38S–43S.
- Nishio H., Otsuka M., Kinoshita S., Tokuoaka T., Nakajima M., Noda Y., Fukuyama Y. and Suzuki K. (2002) Phosphorylation of c-Cbl protooncogene product following ethanol administration in rat cerebellum: possible involvement of Fyn kinase. *Brain Res.* **950**, 203–209.
- Roebuck T. M., Mattson S. N. and Riley E. P. (1998) A review of the neuroanatomical findings in children with fetal alcohol syndrome. *Alcohol. Clin. Exp. Res.* **22**, 339–344.
- Schaefer A. W., Kamiguchi H., Wong E. V., Beach C. M., Landreth G. and Lemmon V. (1999) Activation of the MAPK signal cascade by the neural cell adhesion molecule L1 requires L1 internalization. *J. Biol. Chem.* **274**, 37965–37967.
- Schaefer A. W., Kamei Y., Kamiguchi H., Wong E. V., Rapoport I., Kirchhausen T., Beach C. M., Landreth G., Lemmon S. K. and Lemmon V. (2002) L1 endocytosis is controlled by a phosphorylation-dephosphorylation cycle stimulated by outside-in signaling by L1. *J. Cell Biol.* **157**, 1223–1232.
- Schmid R. S., Pruitt W. M. and Maness P. F. (2000) A MAP kinase-signaling pathway mediates neurite outgrowth on L1 and requires Src-dependent endocytosis. *J. Neurosci.* **20**, 4177–4188.
- Sebastian B. M. and Nagy L. E. (2005) Decreased insulin-dependent glucose transport by chronic ethanol feeding is associated with dysregulation of the Cbl/TC10 pathway in rat adipocytes. *Am. J. Physiol. Endocrinol. Metab.* **289**, E1077–E1084.
- Seiler A. E., Henderson A. and Rubin R. (2000) Ethanol inhibits insulin receptor tyrosine kinase. *Alcohol. Clin. Exp. Res.* **24**, 1869–1872.
- Stratton K., Howe C. and Battaglia F. (1996) *Fetal Alcohol Syndrome: Diagnosis, Epidemiology, Prevention, and Treatment*. National Academy Press, Washington, DC.
- Suvarna N., Borgland S. L., Wang J., Phamluong K., Auberson Y. P., Bonci A. and Ron D. (2005) Ethanol alters trafficking and functional N-methyl-D-aspartate receptor NR2 subunit ratio via H-Ras. *J. Biol. Chem.* **36**, 31450–31459.
- Takeda Y., Asou H., Murakami Y., Miura M., Kobayashi M. and Uyemura K. (1996) A nonneuronal isoform of cell adhesion

- molecule L1: tissue-specific expression and functional analysis. *J. Neurochem.* **66**, 2338–2349.
- Tang N., He M., O’Riordan M. A., Farkas C., Buck K., Lemmon L. and Bearer C. F. (2006) Ethanol inhibits L1 cell adhesion molecule activation of mitogen-activated protein kinases. *J. Neurochem.* **96**, 1480–1490.
- Trowbridge I., Collawn J. and Hopkins C. (1993) Signal-dependent membrane protein trafficking in the endocytic pathway. *Annu. Rev. Cell Biol.* **9**, 129–161.
- Watanabe H., Ymazaki M., Miyazaki H., Arikawa C., Itoh K., Sasaki T., Maehama T., Frohman M. A. and Kanaho Y. (2004) Phospholipase D2 functions as a downstream signaling molecule of MAP kinase pathway in L1-stimulated neurite outgrowth of cerebellar granule neurons. *J. Neurochem.* **89**, 142–151.
- Wisco D., Anderson E. D., Chang M. C., Norden C., Boiko T., Folsch H. and Winckler B. (2003) Uncovering multiple axonal targeting pathways in hippocampal neurons. *J. Cell Biol.* **162**, 1317–1328.
- Yaka R., Phamluong K. and Ron D. (2003) Scaffolding of Fyn kinase to the NMDA receptor determines brain region sensitivity to ethanol. *J. Neurosci.* **23**, 3623–3632.
- Yip P. M., Zhao X., Montgomery A. M. and Siu C. H. (1998) The Arg-Gly-Asp motif in the cell adhesion molecule L1 promotes neurite outgrowth via interaction with the. *Mol. Cell. Biol.* **9**, 277–290.